Observation of Solitary Elastic Surface Pulses

A. M. Lomonosov and P. Hess
Institute of Physical Chemistry, University of Heidelberg, D-69120 Heidelberg, Germany

A. P. Mayer
Institute of Theoretical Physics, University of Regensburg, D-93040 Regensburg, Germany
(Received 17 October 2001; published 1 February 2002)

The formation of solitary elastic surface pulses from laser-generated pulselike initial conditions is reported. The nonlinearity of the medium is compensated by both normal dispersion and anomalous dispersion, which were realized by coating isotropic fused silica by a metal and titanium nitride film, respectively. As an anisotropic material, silicon covered with an oxide layer was studied. The experimental results agree with numerical simulations carried out with a nonlocal evolution equation, which describes nonlinear propagation of surface acoustic waves in a dispersive medium.

DOI: 10.1103/PhysRevLett.88.076104 PACS numbers: 68.35.Ja, 43.25.+y, 43.35.+d, 68.35.Gy

Solitary waves, first observed on the surface of water in a shallow channel, have since been found to exist in various physical systems [1]. Nowadays, they are intensively studied in many branches of science, especially in the field of nonlinear optics because of the prospect of their application in long-distance communication systems based on optical fibers. From the theoretical point of view, solitary waves are spatially localized solutions of nonlinear dispersive evolution equations describing wave propagation in the system. In the case of surface waves on shallow water, this is the celebrated Korteweg–de Vries (KdV) equation, which is integrable via the inverse scattering transform. Its solitary wave solutions possess the soliton property of displaying particlelike behavior when waves collide [1].

While solitary waves on a water surface, which are connected with gravity, were first observed in 1834 and have been thoroughly studied, there has been no clear experimental observation of their elastic counterparts at the surface of a solid. Concerning the shapes and other properties of such solitary surface acoustic waves (SAWs), so far there exist only a few theoretical predictions [2] (for references to earlier work, see [3]). In previous experiments carried out with the aim of detecting signs of solitary surface waves [4–6], a sinusoidal input wave with high amplitude was launched into the system. The recorded waveforms were reminiscent of solitonic structures known to evolve out of sinusoidal initial conditions in the KdV equation [7,8]. However, it was not possible to extract the shape of a single solitary pulse. In fact, the previous experimental results have been largely explained by their authors on the basis of the KdV equation, which is the correct evolution equation for longitudinal bulk waves but not for solitary surface waves. Single longitudinal bulk solitons have been observed recently in plates at 35 K [9], and solitary strain waves in rods are described in [10].

In order to identify a single solitary pulse, it is more favorable to start with a short, high-intensity acoustic pulse. This has been achieved by pulsed laser excitation, a method that has been successfully applied to study nonlinear SAW pulses by monitoring their evolution along the surface of homogeneous elastic media [11–13]. To allow a solitary wave, the elastic nonlinearity of the solid has to be balanced by dispersion. Rayleigh waves become dispersive when the elastic medium is covered by a film with different properties, which gives rise to an acoustic mismatch at the interface. By selecting suitable coatings, both normal and anomalous dispersions were produced to match with the excited nonlinear SAW pulses.

The solitary regime of SAW propagation requires a sufficient amplitude of elastic deformations in the wave field. In experiments with uncoated samples, deformation or acoustic Mach numbers of the order of $M \approx 3 \times 10^{-3}$ are needed to produce an observable nonlinear distortion [12]. A further increase of the SAW magnitude leads to materials fracture and for $M \approx 2 \times 10^{-2}$ the yield strength of most materials is reached. In coated materials, however, the cracking threshold is higher, since shock front formation is suppressed by dispersion.

The experimental setup is shown schematically in Fig. 1. The straight-crested surface pulses were excited

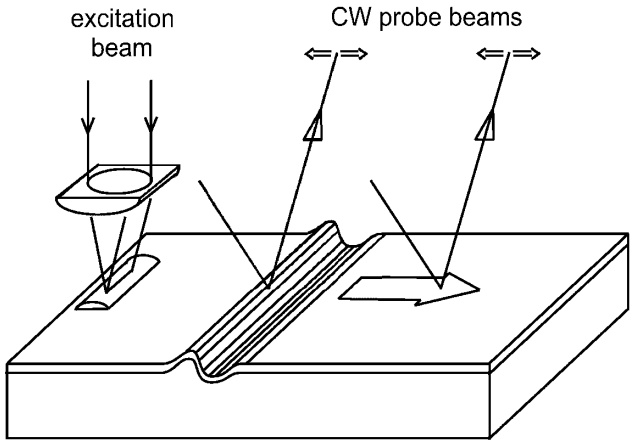

FIG. 1. Experimental setup with exciting laser pulse and cw laser probe-beam deflection.

 © 2002 The American Physical Society

with a Q-switched YAG:Nd laser, operated at 1.064 μm, by focusing the 8 ns long laser pulses to a line of 7 mm length and about 30 μm width. The pulse energy was in the range of 30–60 mJ. For the resulting plane waves the effect of beam diffraction could be neglected for the conditions used. To excite sufficiently nonlinear SAW pulses the absorption layer method was applied [12,13]. In this, the laser radiation is completely absorbed in a thin layer of a highly absorbing carbon suspension that is deposited only in the source region. The explosive evaporation and the resulting recoil momentum exert a high pressure normal to the surface and launch a strong surface pulse.

The traveling pulse is registered by the probe-beam-deflection technique at two probe locations, separated by a fixed distance of 15 mm, using a diode-pumped Nd:YAG laser. The output signal of the position-sensitive detector is proportional to the surface slope $u_{3,1} = \partial u_3/\partial x_1$ in the wave propagation direction, which is related to the particle velocity by $u_{3,1} = -\dot{u}_3/\nu_R$. Here u designates the normal displacement and ν_R is the linear Rayleigh velocity. The wave propagates in the positive direction along the x_1 axis and the x_3 axis is the inward normal to the surface. This setup was used to measure the effect of dispersion for small-amplitude SAWs, the effect of elastic nonlinearity, and both effects simultaneously.

Solitary SAWs differ from solitons on shallow water or in optical fibers in their two-dimensional character. While the latter are guided in a water channel with a depth much smaller than the characteristic spatial extent of the solitary wave in the x_1 direction, or in a spatial region containing the fiber core, solitary surface waves have a nontrivial depth structure. They extend into the medium over depth scales comparable with their width. Nevertheless, a one-dimensional evolution equation for a component $\partial u_\alpha/\partial x = u_{\alpha,1}$ of the displacement gradients at the surface may be derived, where u_α ($\alpha = 1, 2, 3$) are the three Cartesian components of the displacement field.

The elimination of the depth dependence leads to a strongly nonlocal nonlinearity in the corresponding evolution equation [14]. Letting $u_{\alpha,1}(\theta, x_3, X)$ depend on the "retarded time" $\theta = t - x_1/\nu_R$ and a stretched spatial coordinate X along the propagation direction and introducing its Fourier transform yields

$$u_{\alpha,1}(\theta, 0, X) = \int_0^\infty \frac{d\omega}{2\pi}\, e^{-i\omega\theta} U(\omega, X) + \text{c.c.}, \quad (1)$$

where the function $U(\omega, X)$ satisfies the following evolution equation:

$$i\nu_R \frac{\partial}{\partial X} U(\omega) = \omega^2 D(\omega) U(\omega) + \omega \int_0^\omega \frac{d\omega'}{2\pi} F(\omega'/\omega) U(\omega') U(\omega - \omega') + 2\omega \int_\omega^\infty \frac{d\omega'}{2\pi} \left(\frac{\omega}{\omega'}\right) F^*(\omega/\omega') U(\omega') U^*(\omega' - \omega). \quad (2)$$

The dimensionless function F is governed by the second-order and third-order elastic moduli of the substrate material alone, while $D(\omega)$ depends on the acoustic mismatch between the substrate and film of thickness d. $D(\omega)$ may be expanded in powers of $\omega d/\nu_R$. In the following, we retain the zero-order term D_0 only. The evolution equation [Eq. (2)] provides a one-parameter family of solitary wave solutions $u_{\alpha,1}(\theta, 0, X) = \kappa S_\alpha(\kappa[\theta \pm \kappa X])$, with $\kappa > 0$ as the width parameter. The functional form of S_α can be determined numerically as a limiting case of stationary periodic pulse train solutions with periodicity $T = 2\pi/\Omega$, using the ansatz $U(\omega) = \kappa Q_n \exp(\pm i n \Omega \kappa X) \times \delta(\omega - n\Omega)$, with $n = 1, 2, 3, \ldots$, which results in a system of nonlinear algebraic equations for the Fourier amplitudes Q_n. Note that the connection between width, height, and (inverse) velocity of the solitary wave in the frame of reference, moving with the speed ν_R, is the same as for the soliton solutions of the Benjamin-Ono (BO) equation and different from that of the KdV equation.

It follows from the structure of the evolution equation that the integral $\int_{-\infty}^{\infty} d\theta\, u_{\alpha,1}(\theta, 0, X) = u_\alpha(\infty, 0, X) - u_\alpha(-\infty, 0, X)$ vanishes. For isotropic substrates, the function F is real (imaginary) in the case $\alpha = 1$ ($\alpha = 3$). Consequently, the shape of the solitary wave is odd for S_3 and even for S_1. The requirement of a vanishing total area under the pulse leads to a characteristic "Mexican hat" shape of S_1. This is observed for SAW propagation on the Si(100) plane along the ⟨100⟩ direction, too. However, for the propagation geometry Si(111) ⟨112⟩, the function F is neither real nor purely imaginary for either value $\alpha = 1$ or $\alpha = 3$. This results in nonsymmetric pulse profiles. Moreover, in contrast to the situation with the Si(100) cut and

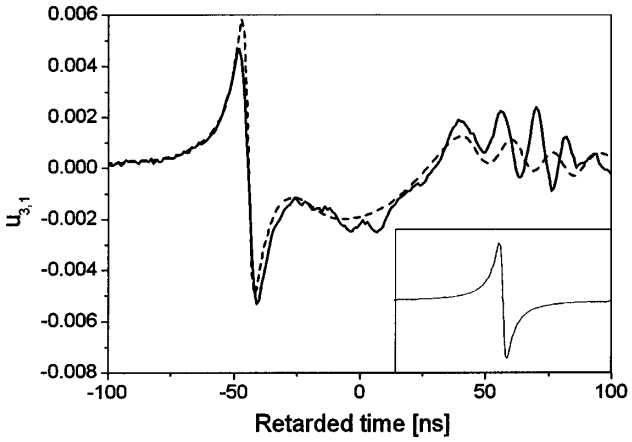

FIG. 2. Evolution of solitary pulse shape for normal dispersion (fused silica with NiCr layer).

the ⟨100⟩ direction, S_3 is an almost even function, while S_1 is approximately antisymmetric. This difference between the two geometries demonstrates the strong influence of the nature of elastic anisotropy of the substrate on the shape of the solitary surface pulses. In the following we consider Eq. (2) only for $\alpha = 3$, which corresponds to the observed quantity $u_{3,1}$.

In systems described by evolution equations with local nonlinearity such as the KdV or BO equation, solitary pulses propagate with a speed higher than the velocity of the nondispersive linear waves for linear normal dispersion. The situation is reversed for anomalous dispersion. The experimental findings and numerical calculations, on the basis of Eq. (2), confirm that this also holds for solitary surface waves in the isotropic systems investigated here.

First we consider the type of nonlinearity observed in isotropic fused silica, which exhibits a nonlinear transformation of the initial surface pulse into a typical U-shaped profile of the normal component of the vibrational velocity for an uncoated medium [11]. This corresponds to the purely imaginary parameter $F(1/2)$ in Eq. (2). The value $F(1/2)$ is associated with the second harmonic generation of a sinusoidal wave and can conveniently be used to describe the character of the nonlinear distortions. Normal dispersion was obtained by deposition of a film consisting of a NiCr alloy (80% Ni, 20% Cr). By numerical simulations employing Eq. (2) it was estimated that a film thickness of about 300 nm was needed to obtain a single solitary pulse at the remote probe location. In the experiments a 300 nm thick film of the NiCr alloy was used. The linear dispersion of a small-amplitude pulse was $\nu_R D_0 = -3.6 \times 10^{-5}$ cm/(s Hz).

The solitary pulse monitored at the remote probe location 17 mm away from the source is depicted in Fig. 2 as a solid line. At the first probe spot a compact pulse of about 20 ns duration was registered. The evolution resulted in the generation of a short bipolar pulse with a speed higher than the linear Rayleigh velocity and in a weak oscillatory tail moving with lower velocity (so-called radiation). Its amplitude is not sufficient for a significant nonlinear effect to occur, and therefore it suffers only the distortions due to dispersion. Consequently, the mean velocity of this wave is lower than the Rayleigh velocity. The theoretical stationary profile $S_3(\theta)$ calculated numerically on the basis of the above equations for this particular case is shown in the inset in Fig. 2. The spatial evolution of the SAW pulse, in fact, leads to the formation of a pulse with the predicted stationary shape.

In the simulations the signal from the first spot was substituted into Eq. (2) as an initial condition. The initial value problem for this equation was solved numerically and the result of the evolution at the remote probe location is shown in Fig. 2 as a dashed line. Since the theory describes the pulse evolution in very good agreement with the experiments it is possible to simulate the further evolution of the solitary pulse. The results are shown in Fig. 3

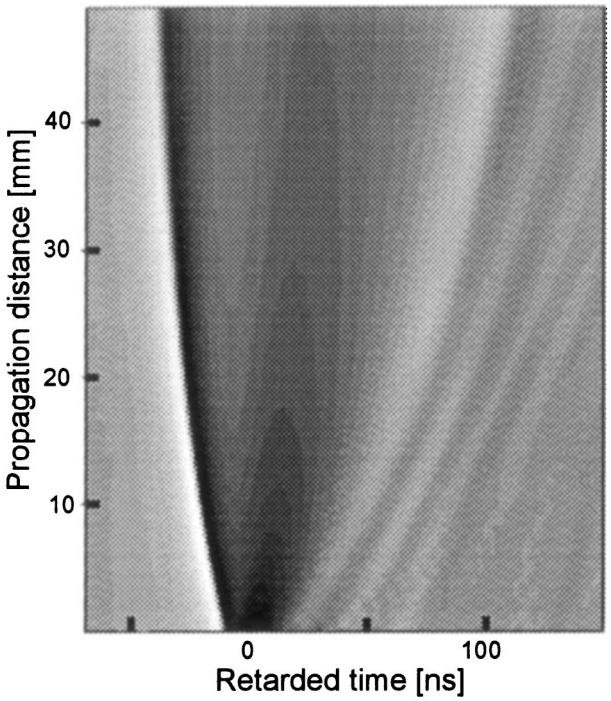

FIG. 3. Simulation of pulse evolution with distance from first probe spot (fused silica with NiCr layer).

in two-dimensional form. Here the propagation distance is plotted versus the retarded time. Note that the distance is given with respect to the first probe spot; hence zero distance corresponds to the profile measured at the first probe spot. Thus the signal depicted in Fig. 2 corresponds in Fig. 3 to a propagation distance of 15 mm. As is evident from Fig. 3, the bipolar pulse essentially conserves its shape, in contrast to the behavior of the oscillatory tail, which significantly broadens with propagation due to dispersion, despite its much narrower bandwidth. The width and velocity of the solitary pulse depend on its amplitude. At the beginning it propagates faster, but as the amplitude decreases due to dissipation, the velocity decreases. The longitudinal velocity component of the signal $u_{1,1}$ is related to the measured $u_{3,1}$ component by the Hilbert transform. Thus the bipolar solitary pulse in the shear component $u_{3,1}$ corresponds to a typical Mexican hat shape in $u_{1,1}$.

To change the sign of the dispersion effect we deposited a "stiffening" film onto a fused silica substrate. As a coating we selected titanium nitride, which possesses a higher stiffness than the substrate. The numerical estimates for the optimal film thickness provided a value of about 50 nm. The measured linear dispersion was $\nu_R D_0 = 1.8 \times 10^{-5}$ cm/(s Hz). From the equations given above it follows that the inversion of D_0 causes the solitary pulse to change its polarity as well. The measurement presented in Fig. 4 confirms this prediction. The profile measured at the remote location behaves with mirror symmetry with respect to the case of normal dispersion: the bipolar solitary pulse has an opposite polarity and a velocity lower than the linear Rayleigh velocity for uncoated fused silica. The

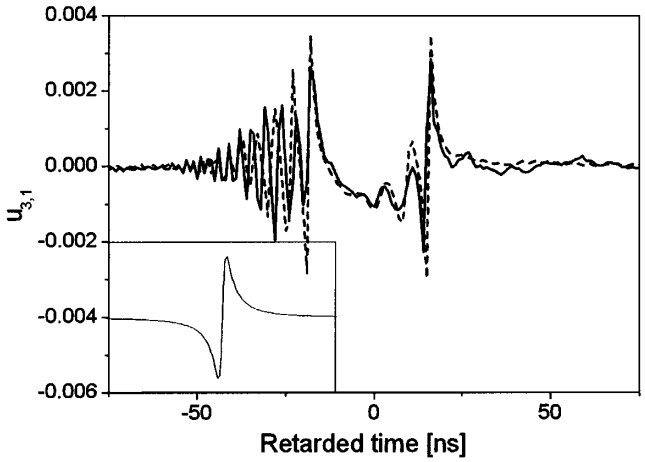

FIG. 4. Evolution of solitary pulse shape for anomalous dispersion (fused silica with TiN layer).

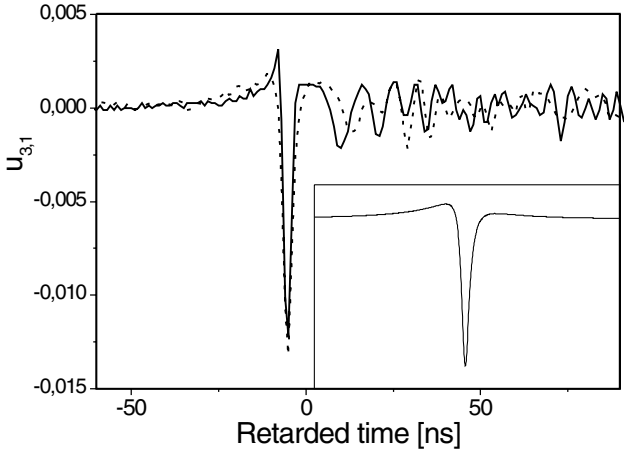

FIG. 5. Evolution of solitary pulse shape for normal dispersion [Si(111) cut with SiO_2 layer].

predicted stationary solution $S_3(\theta)$ is shown in the inset. The numerical simulations were carried out in the same way as for normal dispersion and show satisfactory agreement with the experiment.

The character of nonlinear SAW evolution in crystals can differ essentially from that in isotropic media. For example, nondispersive nonlinear pulse evolution on the Si(111) cut in the $[11\bar{2}]$ direction transforms the short initial pulse into a broadened N-shaped profile [12]. For this direction $F(1/2) = -0.33 - 0.042i$ with the real part dominating. For the wave propagating in the opposite direction $[\bar{1}\,\bar{1}2]$ the parameter $F(1/2)$ changes the sign of its real part, and as a consequence the evolution becomes mirror symmetric with respect to retarded time. For both directions it is the component $S_3(\theta)$ that has a Mexican hat shape in $u_{3,1}$, but the polarities are opposite. To obtain normal dispersion the Si(111) surface was oxidized thermally at 900 °C. The thickness of the silicon dioxide layer was about 110 nm, and the measured dispersion was $\nu_R D_0 = -1.65 \times 10^{-5}$ cm/(s Hz). Solitary pulses with the predicted Mexican hat shapes were observed in the $[\bar{1}\,\bar{1}2]$ direction, as shown in Fig. 5. The solid line shows the experimentally registered pulse and the dashed line shows the prediction of Eq. (2). The inset presents the theoretical stationary solution for this particular system.

In summary, solitary surface elastic pulses have been observed for the first time in a laser-based pump-probe experiment by allowing the two major sources of distortion to compensate each other. The nonlinearity was matched by dispersion generated, respectively, by loading and by stiffening the surface with a thin layer. In the former case the solitary pulses propagated faster than the linear Rayleigh velocity, in the latter more slowly. An evolution equation, which deviates from the KdV equation, containing nonlocal dispersion and nonlocal nonlinearity describes the experimentally observed pulse shapes. This fact stresses the special features of solitary elastic surface waves in comparison to solitary water surface waves and bulk elastic deformation solitons.

We thank C. Eckl for assistance in the numerics and A. S. Kovalev for helpful discussions. Financial support by the Deutsche Forschungsgemeinschaft is gratefully acknowledged.

[1] See, for example, M. Remoissenet, *Waves Called Solitons* (Springer, Berlin, 1994).
[2] C. Eckl, A. P. Mayer, and A. S. Kovalev, Phys. Rev. Lett. **81**, 983 (1998).
[3] A. P. Mayer, Phys. Rep. **256**, 237 (1995).
[4] V. I. Nayanov, JETP Lett. **44**, 314 (1986) [Pis'ma Zh. Eksp. Teor. Fiz. **44**, 245 (1986)].
[5] Y. Cho and N. Miyagawa, Appl. Phys. Lett. **63**, 1188 (1993).
[6] V. Kavalerov, H. Katoh, N. Kasaya, M. Inoue, and T. Fujii, Jpn. J. Appl. Phys. **34**, 2653 (1995).
[7] N. J. Zabusky and M. D. Kruskal, Phys. Rev. Lett. **15**, 240 (1965).
[8] A. Salupere, G. A. Maugin, and J. Engelbrecht, Proc. Est. Acad. Sci. **46**, 118 (1997).
[9] H.-Y. Hao and H. J. Maris, Phys. Rev. B **64**, 064302 (2001).
[10] A. M. Samsonov, *Strain Solitons in Solids and How to Construct Them* (Chapman&Hall/CRC, Boca Raton, 2001).
[11] Al. A. Kolomenskii, A. M. Lomonosov, R. Kuschnereit, and P. Hess, Phys. Rev. Lett. **79**, 1325 (1997).
[12] A. M. Lomonosov and P. Hess, Phys. Rev. Lett. **83**, 3876 (1999).
[13] A. M. Lomonosov, V. G. Mikhalevich, P. Hess, E. Yu. Knight, M. F. Hamilton, and E. A. Zabolotskaya, J. Acoust. Soc. Am. **105**, 2093 (1999).
[14] D. F. Parker and F. M. Talbot, J. Elasticity **15**, 389 (1995); M. F. Hamilton, Yu. A. Il'insky, and E. A. Zabolotskaya, J. Acoust. Soc. Am. **97**, 882 (1995); D. F. Parker and J. K. Hunter, Suppl. Rend. Circ. Mat. Palermo, Ser. II **57**, 381 (1998).